Texture of Crystalline Solids
1979, Vol. 3, pp. 85-112

RECRYSTALLIZATION TEXTURES OF SILVER, COPPER AND α-BRASSES WITH DIFFERENT ZINC-CONTENTS AS A FUNCTION OF THE ROLLING TEMPERATURE

URSULA SCHMIDT and KURT LÜCKE

Institut für Allgemeine Metallkunde und Metallphysik der Technischen Hochschule Aachen, Germany FRG

(Received September 19, 1978)

Abstract: The recrystallization textures of copper and different Cu-Zn alloys as well as the rolling and recrystallization textures of silver of varying purity were investigated as a function of the rolling temperature. In all cases in which the pure copper type rolling texture was present the cube texture was found as recrystallization texture, whereas in the case of the pure brass type rolling texture the brass type recrystallization texture (326)[83$\bar{5}$] developed. In the transition range a large number of well defined and reproducible recrystallization orientations occurred. The high accuracy of the present pole figure measurements allowed a detailed discussion of the results with regard to the mechanisms of formation of the recrystallization textures.

1. INTRODUCTION

The rolling textures of fcc metals have been investigated in many papers.[1] It was found that they possessed either the form of the copper-type rolling texture ("Cu-texture") or the brass-type rolling texture ("Bs-texture"), or consisted of a transition-type in between both ("Tr-texture"). It was further shown that the Cu-texture occurred preferentially at high rolling temperatures with metals and alloys of high stacking fault energy, while the Bs-texture occurred under the opposite conditions.

The recrystallization textures of these metals have been investigated much less thoroughly then the rolling textures and often only in the form of spot check experiments. Here the pole figures exhibited much larger differences than those of the rolling textures. Moreover, although the results of

different authors showed many common features, there were also serious discrepancies. Often insufficient distinction was made between textures resulting from primary recrystallization and from grain growth. In particular the main question was not answered satisfactorily, i.e. whether the (primary) recrystallization texture is determined by the rolling texture only, or whether it is influenced also by other factors.

For these reasons systematic measurements of the primary recrystallization textures of copper-zinc (α-brass) alloys have been carried out in the following work. As in the thorough investigations of the rolling textures of the same alloys by Alam, Mengelberg and Lücke,[2] the zinc content and rolling temperature were systematically varied.

The only *pure* metal (apart from Ytterbium) which forms a Bs-type texture after rolling at room temperature is silver. This means that this metal is of particular interest for deciding whether the recrystallization texture is determined solely by the rolling texture. For this reason and since the textures for this metal were only partly known, some results for rolling and recrystallization textures of silver of different purities and for different rolling temperatures have been included in the present paper.

The investigated textures are represented in the form of pole figures. In order to cover the many alloys and parameters studied in this paper, a very great number of pole figures had to be determined (more than 300). In order to obtain the desired reproducibility, the greatest care had to be taken in the preparation of the specimens and in the measuring technique. The great number of measurements as well as their high quality have been achieved by the use of a high speed, fully automatic texture goniometer*.[2] The results of these investigations were discussed in terms of oriented growth and oriented nucleation. Orientation relationships between deformation and recrystallization textures characterized by a 40° rotation around a common <111>-pole were found to play an especially important role.

2. EXPERIMENTAL METHODS

Quantitative {111} and {200} pole figures were measured with the fully automatic texture goniometer developed by Lücke, Burmeister, Mengelberg and Alam.[2,3] The greatest part of the pole figures (α = 0° to 85°) was measured by the X-ray back reflection method of Schultz,[4] and only for the periphery (α = 75° to 90°) the transmission method of Decker et al.[5] was used. In both regions the countercurrent was automatically corrected with great accuracy with respect to background, diffraction and geometrical errors, then recorded and automatically plotted as a pole figure in form of contour line representations. The intensities were given as multiples of those of Cu- and Ag-powder samples with a random orientation distribution. In general, the error in the quantitative pole figures was approximately ± 10%.

*Now manufactured by Siemens, Karlsruhe, Germany.[3]

The rolled Cu-Zn specimens were etched to a thickness of d = 0.09 mm which correspond to μd = 4 (μ = absorption coefficient for the X-rays) so that the same specimen could be used for both methods. For silver, thick specimens and only back reflection measurements (up to α = 85°) were applied. During all measurements the specimens were subjected to a 12 mm shuttle motion perpendicular to the rolling direction to obtain better averaging.

The Cu-Zn-specimens were the same as used by Alam et al.[2] for the determination of their rolling textures. More detailed information on the specimen production can be found in that paper. The melted Cu-Zn-specimens (purity better than 99.99%) were cold-rolled and annealed to give a uniform grain diameter of 0.05 mm and nearly textureless samples. These were subjected to reversed rolling of 95% (20 to 50 passes) to a thickness of 0.25 mm in a rolling mill (roll-diameter 15 mm) placed in a temperature bath. The following rolling temperatures T_R and liquids were used: -196°C (temperature bath filled with liquid nitrogen); -130°C and -30°C (pentan bath kept at these temperatures by liquid nitrogen running through a cooling pipe); -80°C (solid carbon dioxide with the sublimation temperature -80°C added to the pentan bath) and +20, +60, +130, +200 and +275°C (electrically heated oil bath). The rolled specimens were stored under liquid nitrogen to avoid premature recrystallization (Cu rolled at -196°C has a recrystallization time of 10^6 sec at 20°C, see Figure 1a and Refs. 6 and 7).

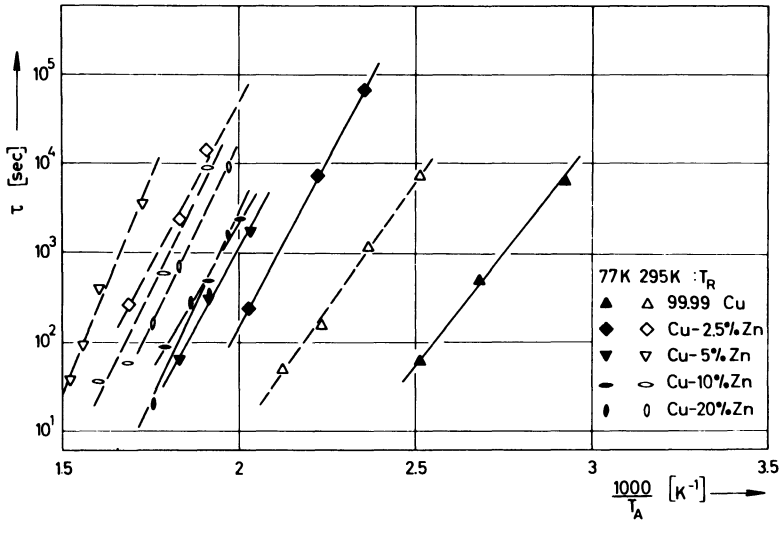

Figure 1a. Times corresponding to half the change of resistivity or hardness during recrystallization as a function of the annealing temperature T_A for Cu 99.99% and various Cu-Zn-alloys rolled 95% at 77°K and 295°K. (The apparent activation energies resulting from this plot lie between 1 and 2 eV.)

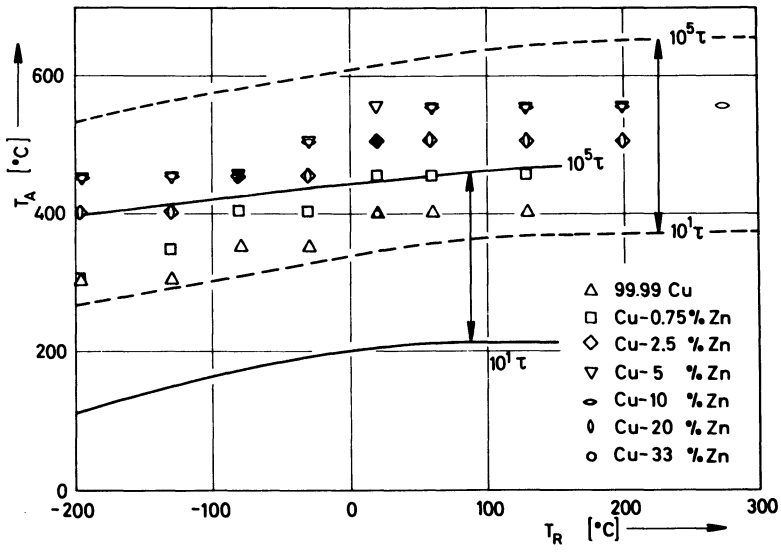

Figure 1b. The symbols indicate the chosen annealing temperatures T_A for Cu 99.99% and various Cu-Zn alloys as a function of the rolling temperature. The full lines (for Cu 99.99%) and the dashed lines (for Cu-10% Zn) indicate the temperature interval in which an annealing treatment of 30 minutes results in the (constant) primary recrystallization texture.

For recrystallization the Cu-Zn-specimens were etched to remove the surface layer, wrapped in thin copper foil to avoid oxidation, and then annealed in air. The annealing temperatures T_A were chosen such that for a fixed annealing time of 30 minutes the primary recrystallization was complete but no appreciable grain growth had taken place. To derive this temperature, measurements of the recrystallization kinetics of this material carried out by Rosenbaum and Lücke[7] were applied. There the times τ which correspond to half the change of resistivity or hardness occurring during recrystallization were measured as a function of the annealing temperature T_A. Figure 1a shows some of these results.

By comparing textures and additional micro-structural investigations with the data from Figure 1a, it could be shown that the rolled specimens were completely recrystallized after annealing times of $10^1\tau$ to $10^2\tau$ and that grain growth occurred only after $10^5\tau$ to $10^7\tau$. Thus from the curves of Figure 1a the temperature ranges could be determined in which the specimens could be annealed for 30 minutes without a change in the recrystallization texture, i.e. in which 30 minutes lies between $10^1\tau$ and $10^5\tau$. They are indicated in Figure 1b for Cu 99.99% (full lines) and for Cu-10%Zn (dashed lines), as examples. Figure 1b also shows the recrystallization temperatures finally chosen such that the annealing time (30 min) was $10^3\tau$ to $10^4\tau$. This recrystallization treatment gave final grain sizes in the range of 0.005-0.05 mm.

For silver purities of 99.99% and 99.999% were investigated. By a proper cold rolling and annealing treatment,

samples were produced which were nearly textureless and had an average grain diameter of 0.01 to 0.03 mm. These samples were subjected to reversed rolling of 95% to 0.15 mm at 20°C or -196°C. (After rolling at -196°C the Ag 99.999% samples are fully recrystallized after 2 hours at 20°C, whereas Ag 99.99% shows the first signs of recrystallization only after 150 days.) After etching off the surface layer the specimens were recrystallized by annealing 30 min in a salt bath. The annealing temperature T_A was determined by hardness measurements. T_A = 250°C after rolling at -196°C and T_A = 350°C after rolling at 20°C were chosen for Ag 99.99%, where temperatures 50°C lower were used for Ag 99.999%. The final grain size was found to lie between 0.005 and 0.015 mm.

3. EXPERIMENTAL RESULTS

3.1 *Cu-Zn-Alloys*

The rolling textures of the Cu-Zn-alloys as a function of Zn-content and rolling temperature have been thoroughly investigated by Alam, Mengelberg and Lücke.[2] Since the same materials and, in some cases, even the same specimens were used in the present measurements of the recrystallization textures, no systematic measurements of the preceding rolling textures were needed. Some spot checks were made which agreed well with the results of Alam et al.[2] Examples of the observed rolling textures are given in Figures 2, 3 and 4.

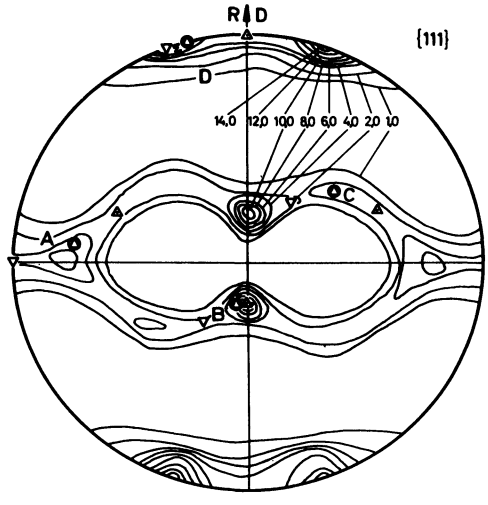

Figure 2. Copper-type rolling texture (Cu 99.99%, rolled at 95% at 20°C). △(112)[11$\bar{1}$], ⓐ(123)[63$\bar{4}$], ▽(011)[21$\bar{1}$].

As with the rolling textures, where the Cu- and Bs-textures occurred as limit cases, two limit types were found for the recrystallization textures: (i) At high rolling temperatures and low Zn-content, the cube texture (001)[100] (Figure 5a and 5b) which often weakly contained the correspond-

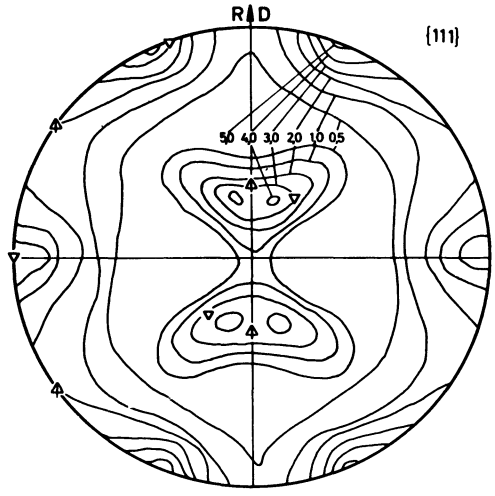

Figure 3. Brass-type rolling texture (Cu-5%Zn, rolled 95% at -196°C). ▽(011)[21$\bar{1}$], ⏃(011)[100].

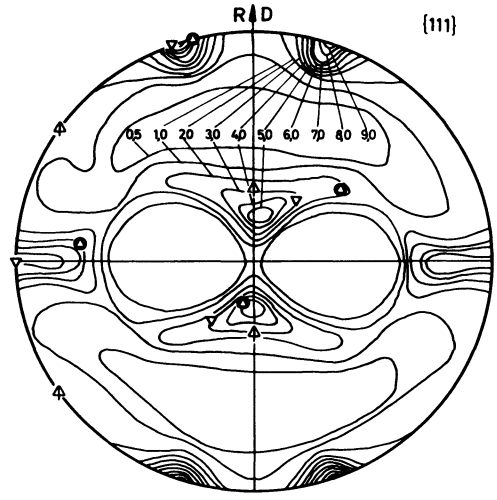

Figure 4. Transition type rolling texture (Cu-5%Zn, rolled 95% at 20°C). ⏃(123)[63$\bar{4}$], ▽(011)[21$\bar{1}$], ⏃(011)[100].

ing twin orientations (122)[21$\bar{2}$], and (ii) at low rolling temperatures and high Zn-content, the brass-type recrystallization texture (Figure 6a/b) which consists of the four components of the ideal orientation (326)[83$\bar{5}$]. As well as the two limit types a great variety of apparently complex transition types were found. Examples of such transition types are shown in Figure 7a/b (Cu 99.99% after rolling at -196°C), Figure 8 (alloys with different Zn-content after rolling at room temperature), Figure 9 (Cu-5%Zn after rolling at different temperatures) and Figure 10 (alloys with different Zn-content after rolling at -196°C.

In spite of their complexity these primary recrystallization textures are reproducible. It proved possible to

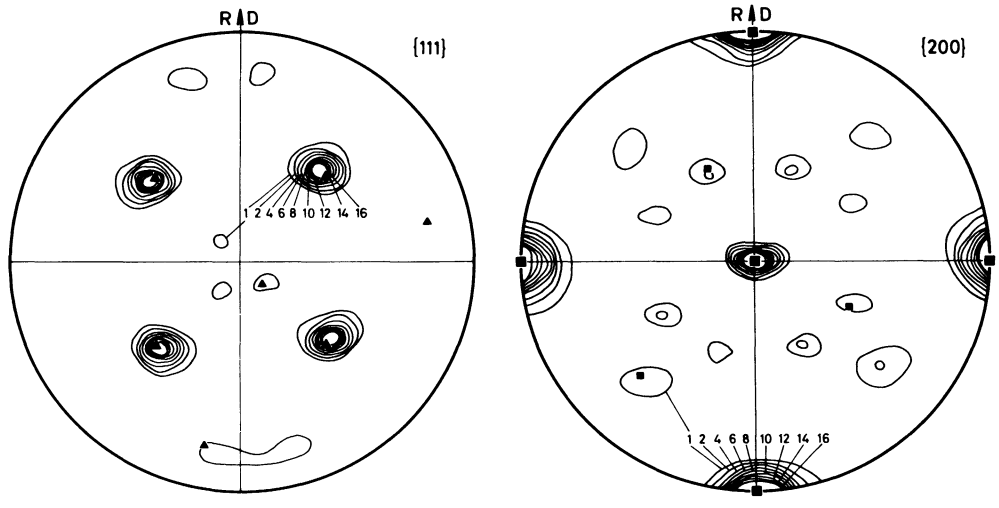

(a) (b)

Figure 5. Recrystallization texture of Cu 99.99%, rolled 95% at 20°C. ▲■(001)[100], ▲■(122)[21$\bar{1}$].

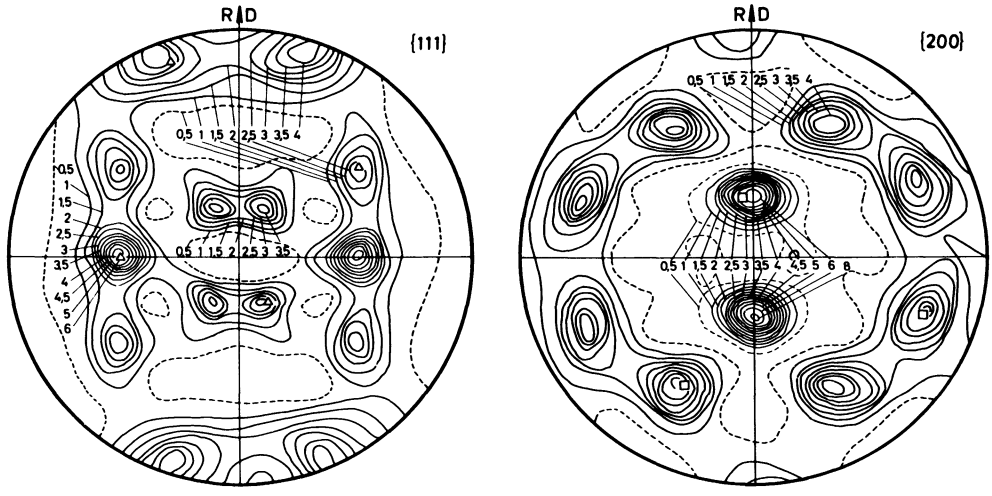

(a) (b)

Figure 6. Recrystallization texture of Cu-20%Zn, rolled 95% at -196°C. △□(326)[83$\bar{5}$].

describe them by 6 ideal orientations which were chosen to fit best to the maxima of the {111} and {200} pole figures. These orientations are indicated in the pole figures by triangles and squares and listed in Table 1. In choosing these orientations, it had to be taken into account that the positions of the maxima differed somewhat in different pole figures and, in cases of low intensity, could even not be exactly defined.

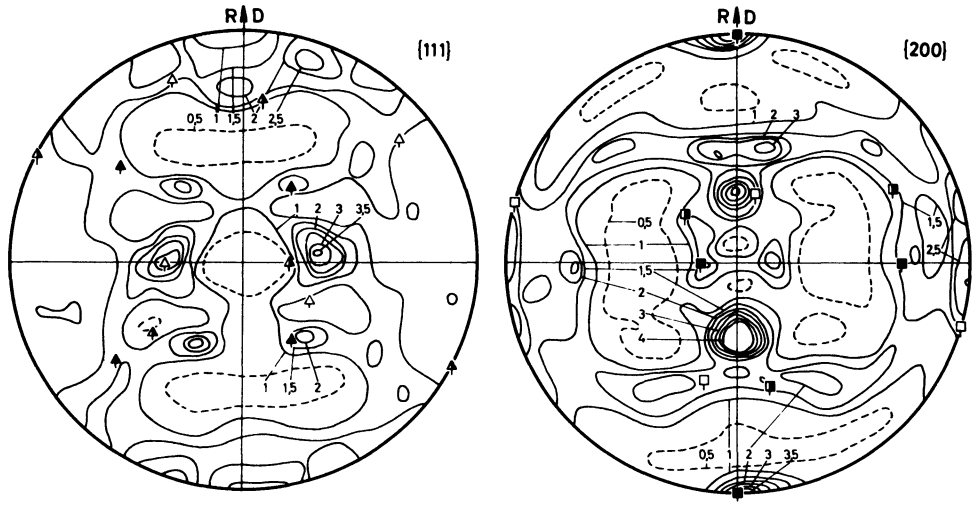

Figure 7. Recrystallization texture of Cu 99.99%, rolled 95% at -196°C. △□(203)[31$\bar{2}$], ▲■(013)[100], ▲□(132)[11$\bar{3}$].

3.2 *Silver*

Neither in the rolling textures nor the recrystallization textures of silver could difference be detected between the two different purities used in this investigation. For this reason only the pole figures of Ag 99.999% are displayed. Figures 11a/b and 12a/b give the rolling textures after rolling at -196°C and 20°C; both are of the Bs-type. Figures 13a/b and 14a/b show that the corresponding recrystallization texture after rolling at -196°C was of the pure (326)[83$\bar{5}$]-type, whereas after rolling at 20°C the orientation (013)[100] was additionally found.

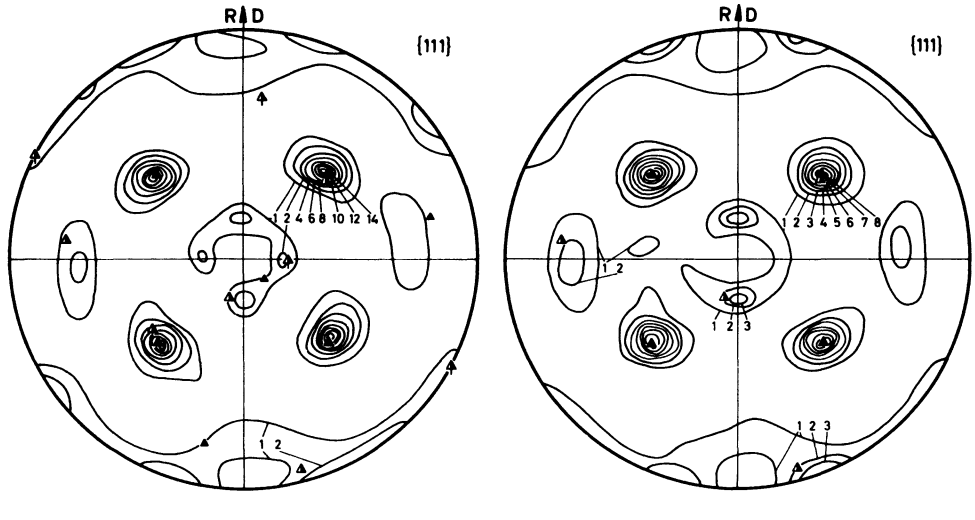

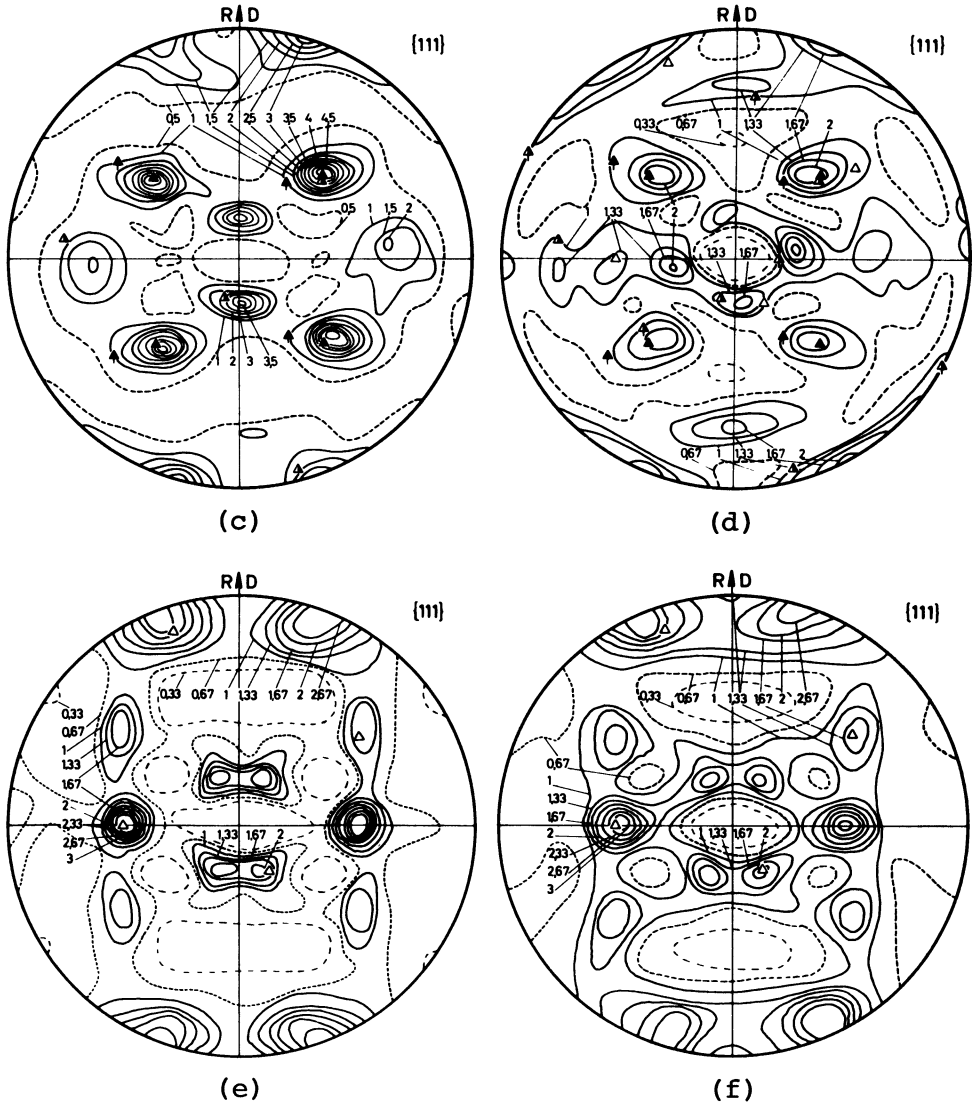

Figure 8. Recrystallization texture of Cu-Zn alloys rolled 95% at 20°C. (a) Cu-0.75%Zn, (b) Cu-2.5%Zn, (c) Cu-5%Zn, (d) Cu-10%Zn, (e) Cu-20%Zn. ▲(001)[100], ▲(122)[21$\bar{1}$], ◭(368)[42$\bar{3}$], ▲(013)[100], ◭(132)[11$\bar{3}$], △(326)[83$\bar{5}$].

4. DISCUSSION OF THE RESULTS

4.1 *Rolling Textures*

From the electron diffraction measurements on single grains in some Cu-Zn-alloys by Perlwitz, Lücke and Pitsch[8] together with the determination of 3-dimensional orientation distribution functions (ODFs) by Pospiech and Lücke[9] and Schmidt, Lücke and Pospiech[10] it has been shown that the rolling textures of the fcc-metals are composed of the 3 main orientations (011)[21$\bar{1}$], (123)[63$\bar{4}$] and (112)[11$\bar{1}$]. Additionally,

Table 1. Orientation distance ρ between recrystallization orientations and 40° (30°) <111> rotated rolling orientations. - indicates ρ > 25°. In addition, pole (A,B,C,D) and sign (+,-) of rotation are shown.

Rolling Orientation	(011)[21$\bar{1}$]		(123)[63$\bar{4}$]				(112)[11$\bar{1}$]		(011)[100]
Recrystallization Orientation	Comp. I	Comp. II	Comp. I	Comp. II	Comp. III	Comp. IV	Comp. I	Comp. II	Comp. I
(001)[100]	B+ = C+	B+ = C+	C+	C+	C+	C+	A- = C+	A- = C+	
(cube orientation)	23°(-)	23°(-)	10°(20°)	10°(20°)	10°(20°)	10°(20°)	23°(-)	23°(-)	- (-)
(368)[42$\bar{3}$]	D+ = D-	A+ = A-		B-	D-	A+	B+ = B-	D+ = D-	B± = C±
(R-orientation)	22°(13°)	18°(-)	- (-)	15°(14°)	5°(9°)	13°(20°)	22°(13°)	16°(23°)	18°(20°)
(132)[11$\bar{2}$]	B- = C-			D+	C-	D+	D+ = D-	A+ = C-	A± = D±
(asym. orientation)	25°(20°)	- (-)	- (-)	22°(-)	12°(3°)	21°(21°)	20°(21°)	20°(16°)	8°(13°)
(013)[100]	B+ = C+	B+ = C+	C+	C+	C+	C+	A+ = C-	A+ = C-	B± = C+
(tilted cube orient.)	8°(17°)	8°(17°)	14°(17°)	24°(-)	24°(-)	14°(17°)	23°(-)	23°(-)	- (25°)
(203)[31$\bar{2}$]	D+ = D-	B- = C-	B-	D+	C-	D+	D+ = D-	D+ = D-	A± = D±
(Cu-low temp. orient.)	15°(25°)	16°(17°)	- (25°)	12°(13°)	17°(17°)	12°(20)	-(23°)	23°(23°)	17°(-)
(326)[83$\bar{5}$]	D+ = D-	B- = C-	D+	B-	D-	A+	A- = C+	D+ = D-	B± = C±
(Br-recryst.orient.)	7°(9°)	8°(15°)	23°(13°)	10°(10°)	19°(-)	20°(-)	- (20°)	23°(-)	20°(25°)
(211)[01$\bar{1}$]	A+ = A-	A+ = A-	A-	A+	A+	A-			
(unobs.recryst.o.)	10°(0°)	10°(0°)	19°(19°)	24°(19°)	24°(19°)	19°(19°)	- (-)	- (-)	- (-)

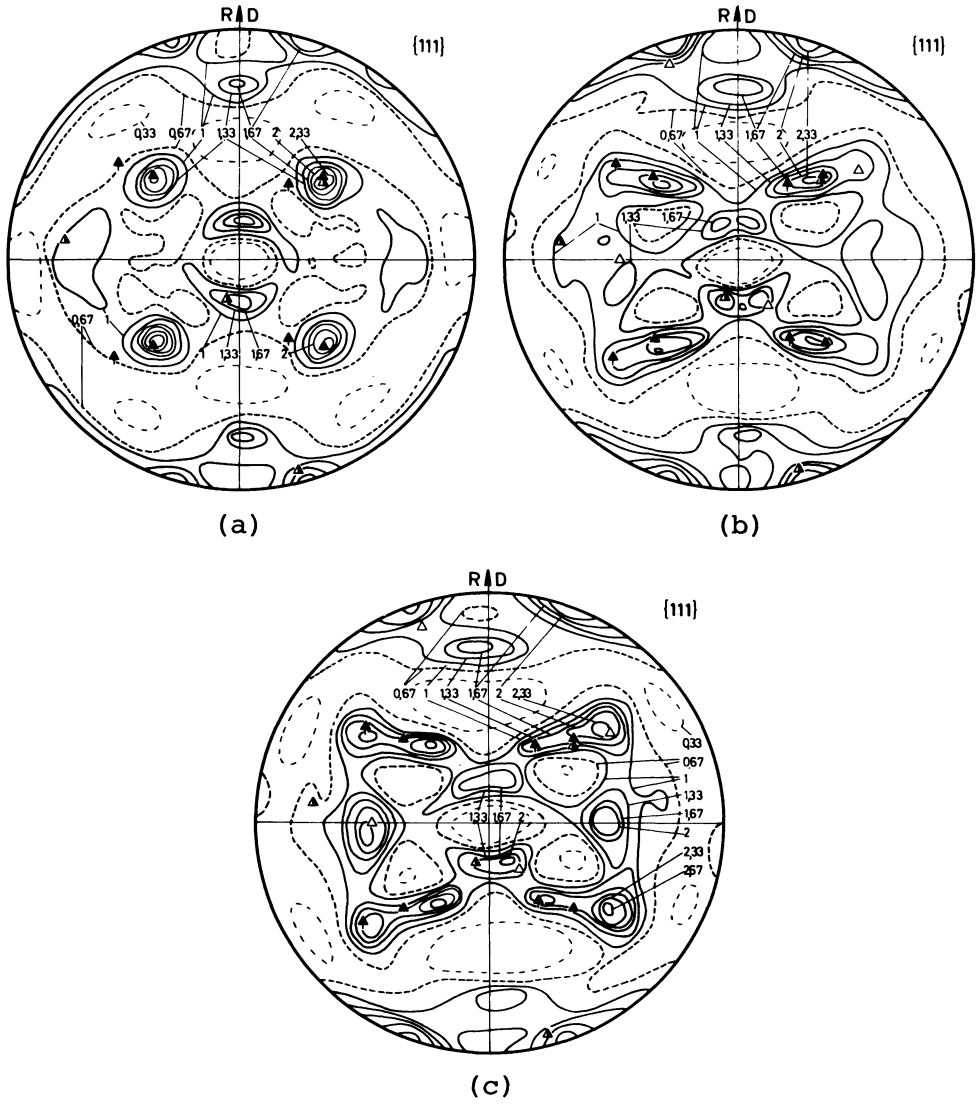

Figure 9. Recrystallization textures of Cu-5%Zn, rolled 95% at different temperatures. (a) -30°C, (b) -80°C, (c) -130°C. ▲(001)[100], ◭(368)[42$\bar{3}$], ▲(013)[100], △(326)[83$\bar{5}$].

in the Tr- and Bs-type rolling textures the Goss-orientation (011)[100] was found, and in the Cu- and Tr-type (not in the very pure Bs-type) rolling textures a small amount of the tilted cube orientation (013)[100] was observed. By examining the characteristic positions in the {111} and {200} pole figures of Alam et al., the present authors have estimated the volume fractions of the 4 main components contained in the rolling textures. The results are given in Figure 15a. The heavy zig-zag-line characterizes the texture transition. Examples for the pole figures with and without the Goss-orientation are given in Figures 3 and 4 and in Figure 2, and with and without the (013)[100] orientation in Figure 12 and in Figure 11, respectively.

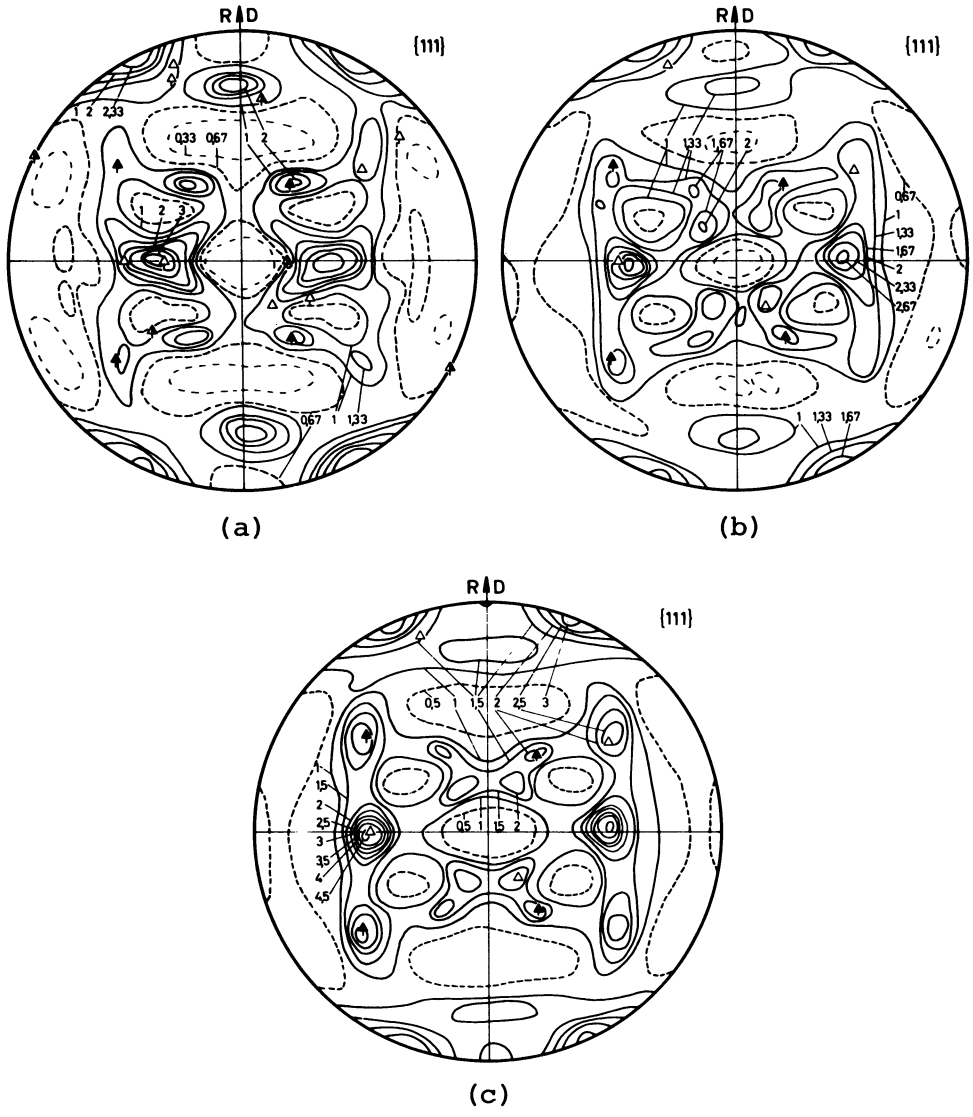

Figure 10. Recrystallization textures of Cu-Zn alloys, rolled 95% at -196°C. (a) Cu-0.74%Zn, (b) Cu-2.5%Zn, (c) Cu-5%Zn. △(203)[31$\bar{2}$], ▲(132)[11$\bar{3}$], ▲(013)[100], △(326)[83$\bar{5}$].

Although it is known that the transition from the Cu-type to the Bs-type rolling texture is caused by the formation of deformation twins,[1] no well founded quantitative theory exists to explain dependence of the transition rolling temperature T_{TR} on alloy content. As already discussed,[2] it is best described by the empirical expression $\tau_{III}(T_{TR})/G = K$ where τ_{III} is the shear stress for the initiation of cross-slip at the temperatures T_{TR} and K is a constant. Since for Cu-alloys $K = 1.1 \times 10^{-3}$,[2] and for silver $K = 0.9 \times 10^{-3}$,[11] an expression of the type $\tau_{III}(T_{TR})/G \approx 10^{-3}$ might be expected to determine generally the transition temperature of the rolling textures.

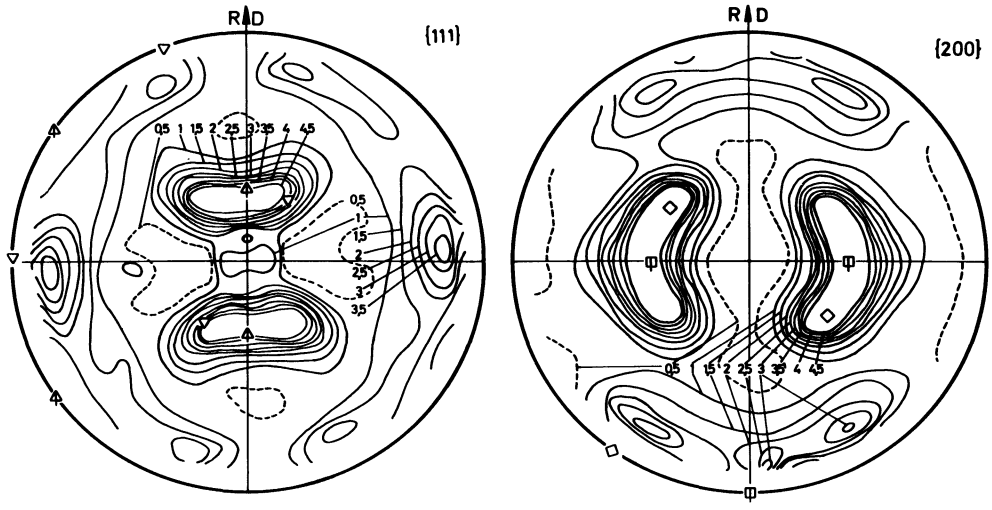

Figure 11. Rolling texture of Ag 99.999%, rolled 95% at -196°C. ▽◇(011)[2$\bar{1}$1], ⏃⏄(011)[100].

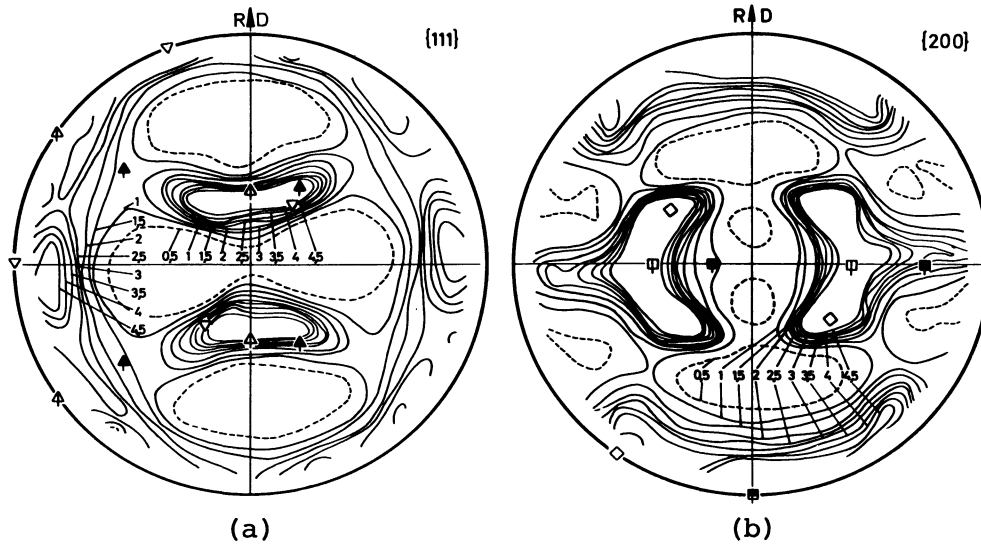

Figure 12. Rolling texture of Ag 99.999%, rolled 95% at 20°C. ▽◇(011)[2$\bar{1}$1], ⏃⏄(011)[100], ▲■(013)[100].

4.2 *Recrystallization Textures*

The recrystallization textures of Cu-Zn-alloys given in the literature, although having mainly the character of spot checks, agree well with the present more complete set. This is the case for the textures determined by Merlini and Beck[12] and Beck and Hu[13] for several different alloys rolled at room temperature. At low Zn-content the (013)[100] orientation was found as well as orientations close to (368)[42$\bar{3}$] and (132)[11$\bar{2}$].[12] For Cu-30%Zn the texture (225)[73$\bar{4}$] has

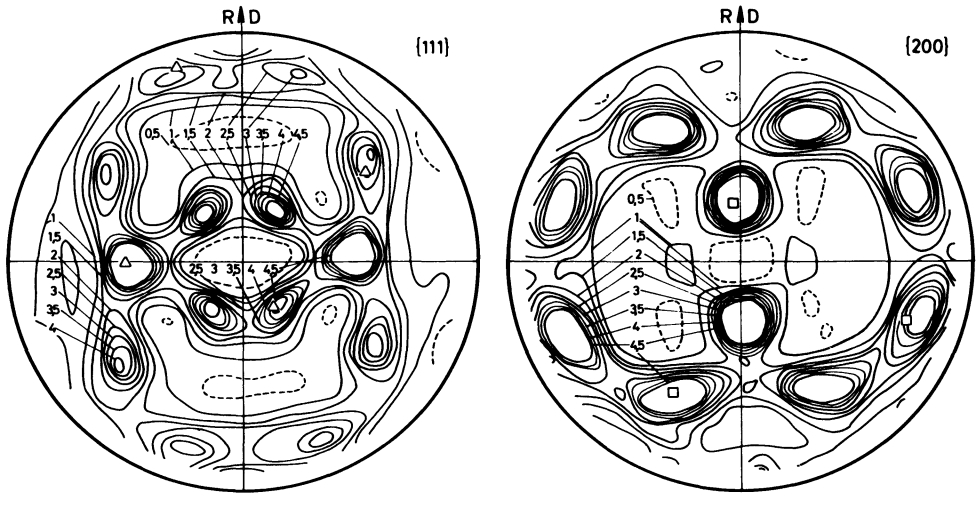

Figure 13. Recrystallization texture of Ag 99.999%, rolled 95% at -196°C. △□(326)[83$\bar{5}$].

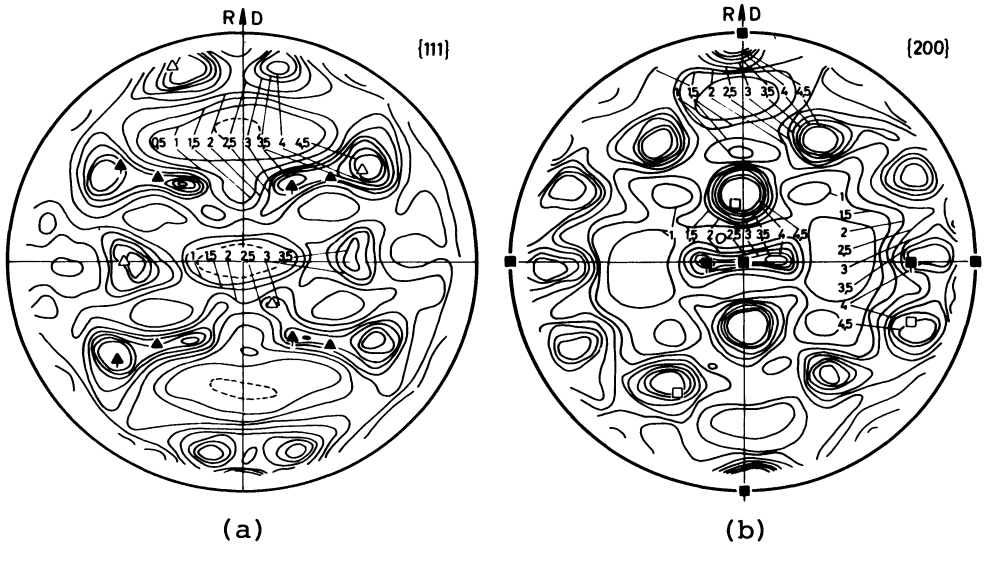

Figure 14. Recrystallization texture of Ag 99.999%, rolled 95% at 20°C. △□(326)[83$\bar{5}$], ▲■(013)[100], ▲■(001)[100].

been reported.[13] This orientation agrees moderately well with the present one (326)[83$\bar{5}$] (within 6°), but their {111}-pole figure looks quite different from that given in Figure 8f. As shown by Lücke and Schmidt,[14] this discrepancy is not caused by a difference in the true texture but by the less accurate texture determination.[13] By decreasing the rolling temperatures for Cu 99.98% Hu and Goodman[15] also obtained transition type recrystallization textures with the orientations (013)[100] and (214)[52$\bar{3}$]. However, the transition

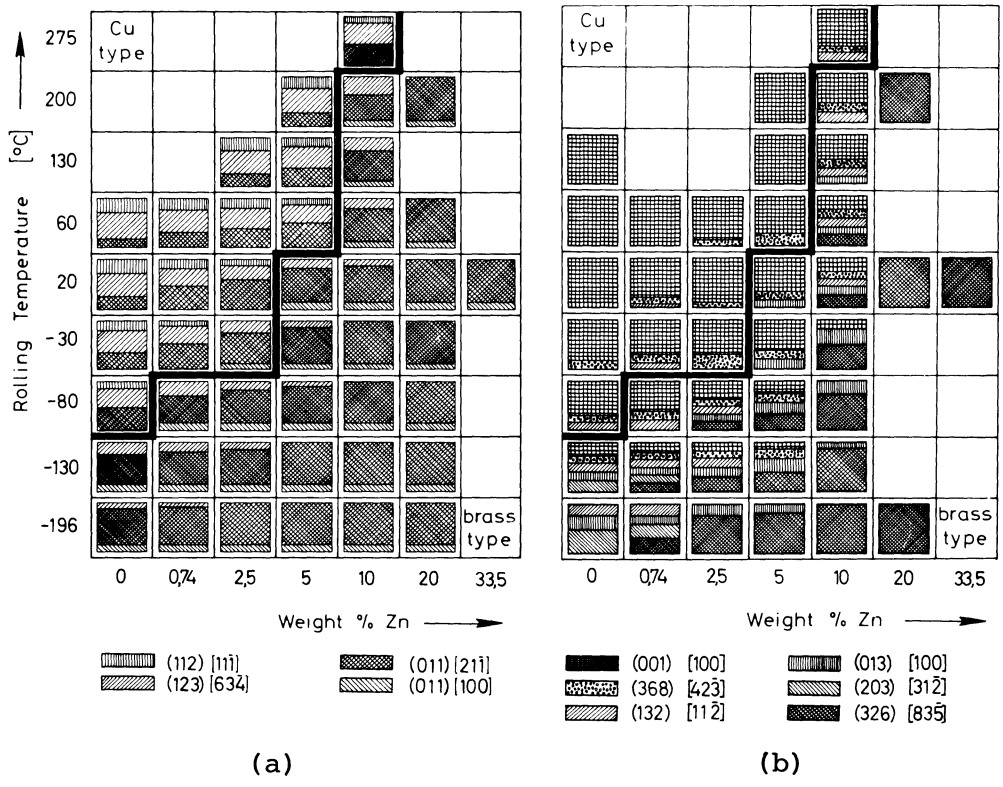

Figure 15. Schematic representation of the textures of the Cu-Zn-alloys as a function of the rolling temperature and the Zn-content. (a) rolling textures, (b) recrystallization textures.

range was shifted to *lower* temperatures compared to the present work.

Also for copper rolled at -196°C their recrystallization texture was not identical with the present one. These observations can be explained by the fact that their rolling mill was not placed in a temperature bath. Instead, the samples were cooled to the intended "rolling temperature" and then rolled at room temperature, so that the true temperature during rolling would probably be higher than given in their paper.

Also for the recrystallization textures, the volume fractions of the different components were estimated by inspecting the characteristic positions of the pole figures. The results are given in Figure 15b as a function of Zn-content and rolling temperature. The heavily drawn step line of Figure 15a indicating the transition from the Cu-type to the Bs-type rolling texture is also shown in Figure 15b. It is recognized that in the latter it also characterizes the texture transition, namely from the cube orientation (001)[100] to the Bs-recrystallization orientation (326)[83$\bar{5}$]. This suggests that, to a first approximation, the recrystallization texture is determined by the rolling texture. Further it is clear that the textures characterized by a great variety of

orientations lie below the step line. This indicates that the pure Bs-recrystallization orientation (326)[83$\bar{5}$] can only form if the rolling texture is of the pure Bs-type, and that the cube orientation becomes strong if all the three main rolling orientations are well developed. It is important to note that the transition from the cube texture to the Bs-type recrystallization texture is not continuous as it is with the rolling textures where, going across the diagram, one component increases at the expense of another. Instead, here in the transition range, many new orientations are formed (up to 4 in one pole figure) with a total volume fraction much higher than that of the 2 extreme orientations. With Cu rolled at -196°C the two extreme orientations do not occur at all. Here the strongest component is the (203)[31$\bar{2}$] orientation which is similar to the Bs-recrystallization orientation.

For silver rolled at -196°C the pure Bs-recrystallization texture (326)[83$\bar{5}$] is found. This is the first time that this texture, which was reported previously only for various Cu alloys, has been found for a pure metal. After rolling at room temperature a texture composed of the orientations (326)[83$\bar{5}$], (013)[100] and (001)[100] was observed. This is a recrystallization texture of the transition type as obtained, for example, also for Cu-5%Zn after rolling at -130°C (Figure 9c)

This texture found in Ag after room temperature rolling does not agree in all points with the equivalent ones given in literature. Hu, Cline and Goodman[16] found with Ag 99.999% the orientations (102)[21$\bar{1}$] and somewhat weaker (013)[100]. These 2 orientations were observed in the present work with Cu 99.99% after rolling at -196°C (Figure 7a/b), i.e. this texture also corresponds to the transition type recrystallization textures for Cu-Zn. For less pure Ag the same authors found a different recrystallization texture which is rather similar to the present Bs-type recrystallization texture. This is in contrast to the present investigation where no influence of small amounts of impurities was found. Slakhorst[17] describes the recrystallization texture of Ag 99.999% after rolling 99.5% at 20°C by the 3 orientations (285)[42$\bar{5}$], (418)[74$\bar{4}$] (9° from (326)[83$\bar{5}$]) and (013)[100], the last 2 of them being in agreement with the present results.

These differences in the results of the various investigations, particularly in the influence of the degree of purity, shall be assumed to be caused by the nature of the main impurities. As shown for Cu-P[10,18], very small additions of high valency elements can shift the recrystallization texture towards the alloy-type.

5. DISCUSSION OF THE MECHANISMS OF FORMATION OF RECRYSTALLIZATION TEXTURES

5.1 *Oriented Growth*

According to Beck,[19] recrystallized grains with certain special orientation relationships to the deformed matrix grow faster than the others and thus determine the recrystal-

lization texture. In fcc single crystals this maximum growth rate ("MGR") orientation was found to be determined by a 40° rotation around a common <111>-axis.[20-23]* In polycrystalline metals the growing grains must be able to grow into several deformed grains with different orientations. This means that the so-called "compromise orientations"[24,25] should be formed rather than the exact MGR-orientation.

In order to examine these predictions, the orientation relationships between one component of each of the observed 6 recrystallization orientations and all components of the 4 rolling orientations (see Sec. 4.1) are considered in Table 1. For this purpose each rolling component was rotated +40° and -40° around each of the 4 <111>-axes (marked in Figure 2 with the letters, A,B,C.D so that 2 × 4 = 8 rotations were obtained for each rolling component. Then the "orientation distances" were determined** between these 40° <111> rotated rolling components and one of the (crystallographically equivalent) components of the particular recrystallization orientation. The smallest of these 8 ρ-values is listed in Table 1 together with the corresponding rotation axis and sign of rotation. A small ρ-value means that the particular rolling components can be transformed readily into the particular recrystallization orientation by such a 40° <111> rotation. The ρ-values based on 30° instead of 40° <111> rotations are given in Table 1 in parentheses beside the 40°-ρ-values. They are generally larger than the values obtained after 40° rotations.

The conclusions from this table, some of which have already been considered by Beck et al.,[24,27] Dillamore[28] and Lücke et al.,[25] will now be discussed in detail. The 40° <111>-relationship will be considered to be well satisfied with $\rho \leqslant 10°$ and fairly well satisfied with $\rho \leqslant 18°$. In addition to the 6 observed recrystallization orientations, the orientation (211)[01$\bar{1}$] which has never been observed is listed in Table 1.

(a) *Brass type rolling texture*. Since this texture consists mainly of two (011)[2$\bar{1}$1]-type components (Figure 16a) only 4 instead of 8 crystallographically not equivalent 40° <111> rotations are obtained (A+ ≡ A-, Figure 16d; B+ ≡ C+, Figure 16c; B- ≡ C-, Figure 16b and D+ ≡ D-, Figure 16b). This Bs-texture has the peculiar property that for each 40° <111> rotation with respect to one component a 40° <111> rotation with respect to the other component exists which leads to nearly the same orientation. Thus by these 40° <111> rotations 3 orientations (shown in Figure 16b,c,d) are obtained which should be able to grow readily into *both* rolling components. These orientations are (326)[83$\bar{5}$] (Figure 16b) and (013)[100] (Figure 16c) which have been observed (cf. Sec. 4.2)

*This orientation relationship will be considered here as an empirical result and the physical reason for the high mobility (which is connected with the structure of the grain boundary) will not be discussed.

**is the largest of the 4 angles between the corresponding {111}-poles of the two orientations and is similar to the disorientation.[26]

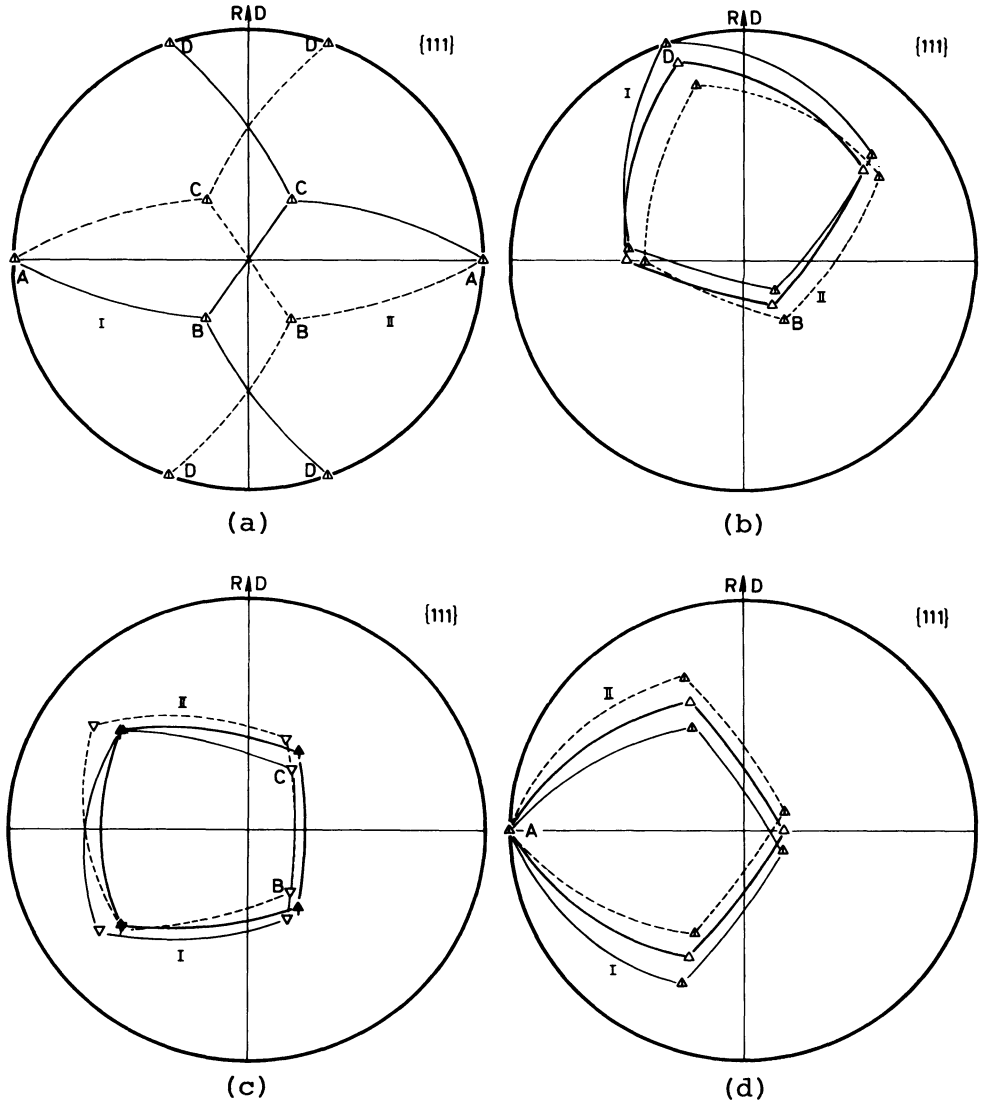

Figure 16. ±40° <111> rotations of both components of (011)[2$\bar{1}\bar{1}$]. (a) ⧋ (full lines) = (011)[$\bar{2}\bar{1}$1] component I and ⧋ (dashed lines) = (011)[$\bar{2}$1$\bar{1}$] component II. (b) ⧋ (011)[2$\bar{1}\bar{1}$] after 40° <111> rotations, component I rotated D+, component II rotated B-, △ (heavy full lines) = (326)[83$\bar{5}$]. (c) ▽ (011)[2$\bar{1}\bar{1}$] after 40° <111> rotations, component I rotated B+, component II rotated C+, ▲ (heavy full lines) = (013)[100]. (d) ⧋ (011)[2$\bar{1}\bar{1}$] after 40° <111> rotations, component I and II rotated A+, △ (heavy full lines) = (211)[01$\bar{1}$].

and the orientation (211)[01$\bar{1}$] (Figure 16d) which has never been observed. According to Table 1 the 40° <111> relationship is satisfied well for these 3 orientations and satisfied fairly well for (203)[31$\bar{2}$] (which is similar to (326)[83$\bar{5}$]).

(b) *Transition type rolling texture*. Here one has to consider, in addition to the (011)[2$1\bar{1}$]-orientation, the 4 components of the S-orientation (123)[6$3\bar{4}$]. Each of these components leads to 8 crystallographically not equivalent rotations. It is well known that the best compromise orientation is the cube orientation (001)[100], (the rotation C+ around all 4 components leads to ρ = 10°, Figure 17a). The

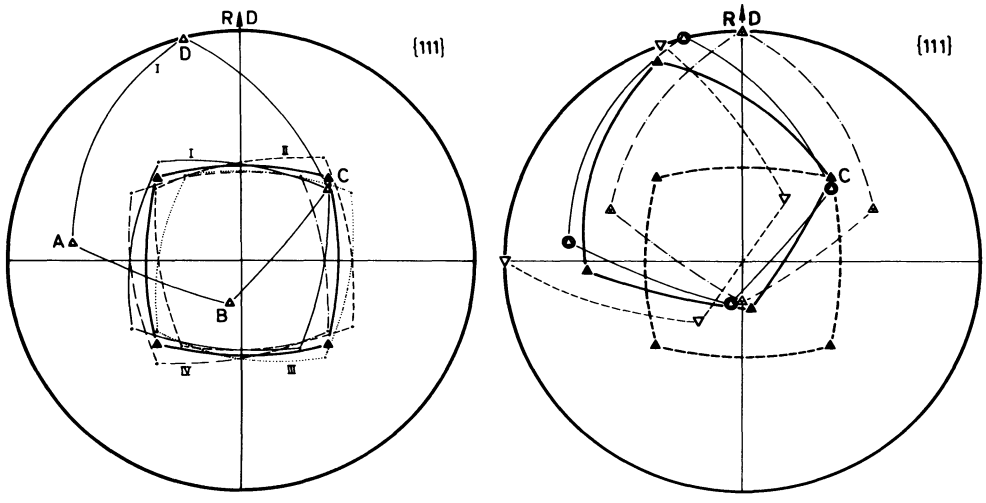

(a) (b)

Figure 17. Orientation relationship between the cube orientation (00$\bar{1}$)[100] and the 3 main rolling orientations (011)[2$1\bar{1}$], (123)[6$3\bar{4}$] and (112)[11$\bar{1}$].
(a) ▲ (heavy full lines) = (001)[100]; △ (123)[6$3\bar{4}$] component I; line systems around (001)[100] = component I-IV of (123)[6$3\bar{4}$] rotated +40° around C.
(b) ▲ (heavy broken lines) = (001)[100]; ▲ (heavy full lines) = (001)[100] rotated +40° around C; ▽ ⓐ △ (light dashed, full and dashed dotted lines) = rolling orientations (011)[2$1\bar{1}$], (123)[6$3\bar{4}$], (112)[11$\bar{1}$].

(368)[4$2\bar{3}$] orientation which is similar to the S-orientation and comparable to the R-orientation found as a recrystallization orientation of aluminium has a fairly good 40° <111> relationship to the other 3 components of the S-orientation. Also the (203)[3$\bar{1}$2]-orientation has a fairly good 40° <111> relationship to 3 components of the S-orientation (as well as to both components of the (011)[2$1\bar{1}$] orientation). The orientations (013)[100] and (326)[83$\bar{5}$], both being favourably oriented with regard to (011)[2$1\bar{1}$], have a fairly good 40° <111> relationship to 2 or one of the 4 components of the S-orientation respectively. The (132)[11$\bar{2}$] orientation has this relationship to only one component.

(c) *Copper type rolling texture*. This rolling texture contains additionally the orientation (112)[11$\bar{1}$] which is composed of only two components thus giving only 4 crystallographically not equivalent 40° <111> relations (A+ ≡ C-,

A- ≡ C+, B+ ≡ B-, D+ ≡ D-). Except for the (368)[42$\bar{3}$] orientation with respect to only one component, there is no 40° <111> relationship within ρ 18°. This means that none of the observed recrystallization orientations should be able to grow well into this rolling component. The growth of the cube orientation is probably due to its fairly good orientation relationship to the 4 components of the S-orientation and to its high symmetry which automatically makes it a compromise (although not a very good one) with respect to the crystallographically equivalent components of the other two orientations (Figure 17b).

Thus the attempts to interpret the observed recrystallization textures on the basis of MGR- and compromise orientations can be summarized as follows:

(i) The main components all have a 40° <111> relationship with respect to the deformed matrix and can easily be interpreted as high growth rate compromise orientations. These are the (326)[83$\bar{5}$] and (013)[100] orientations (and possibly (203)[31$\bar{2}$]) in the case of the Bs-type rolling texture and the cube orientation (001)[100] (and possibly (368)[42$\bar{3}$]) in the case of the Tr-type and Cu-type rolling textures.

(ii) The formation of the (132)[11$\bar{2}$] and the (203)[31$\bar{2}$] orientations in the case of the Tr-type and Bs-type rolling textures cannot be understood since much better compromises exist.

(iii) It cannot be understood why, compared with (326)[83$\bar{5}$], the (013)[100] orientation is only weakly formed and (211)[01$\bar{1}$] not at all, although both would be good compromises (Figures 16c and 16d).

Considering the last point, it has been proposed that the small amount of Goss orientation (011)[100] present in the Bs-type rolling texture suppresses the (211)[01$\bar{1}$][24] and the (013)[100][28] orientations since the ρ-values resulting for these two orientations (ρ = 32° in both cases) are large compared to ρ = 20° for (326)[83$\bar{5}$]. This argument, however, does not explain why the (013)[100] orientation is sometimes found (even with Goss-orientation present in the rolling texture, Figure 15a), but never the (211)[01$\bar{1}$] orientation. Furthermore, the (013)[100 orientation is observed in Ag after rolling at 20°C but not after rolling at -196°C, although the fraction of the Goss orientation in both rolling textures is similar.

5.2 *Oriented Nucleation*

As shown above, some orientations fitting well to 40° <111> and corresponding compromise orientations have not been found in the recrystallization textures, whereas less well fitting orientations are often observed. This shows that still other selection principles for the recrystallization orientations must exist. The extent to which the availability of nuclei could play a role will now be discussed. Nucleation means the production of sufficiently large strain free regions having a favourable orientation difference with respect to the main orientations of the deformed matrix. Three possible mechanisms will be considered.

(a) *Nuclei as parts of the deformed matrix.* This concept of pre-formed nuclei was first proposed by Burgers[29] and was considerably elaborated by Dillamore and Katoh,[30] who systematically considered the orientation differences developing in a crystal during glide. A direct verification of this concept for rolled and recrystallized Al-single crystals was recently given by Lücke, Rixen and Senna[31] and discussed by Hansen, Mecking and Lücke.[32] Dellamore and Katoh[30] assumed that, except for grain boundaries, the nuclei are mainly formed in regions with very strong and very small lattice curvature, i.e. in those parts of the deformed matrix where the orientation change during edformation is especially slow. By applying the Taylor theory, they demonstrated that these orientations form convergent and divergent planes in the orientation space, and found that most of the observed recrystallization orientations lie on or close to these planes. They concluded further that the crystallographic orientation relationship betwen deformation and recrystallization textures (and thus the recrystallization orientations (100)[001] and (326)[83$\bar{5}$] are determined only by the orientations of the nuclei, i.e. of these planes, and not by a subsequent growth selection. However, as already discussed in part by Lücke,[25] this latter conclusion does not appear to be justified:

(i) It is not clear why only a few points of these planes --namely those corresponding to the observed recrystallization orientations--are distinguished to lead to nucleation. Also if one concedes a certain (although much slower) flow of orientations within these planes, it is still not explained why just the orientations characterized by the 40° <111> compromise relationships are the only ones to act as nuclei, whereas other orientations lying within these planes do not.

(ii) This 40° <111> relationship has been found after very different types and degrees of deformation.[25,31,33] Since these different deformations lead to different orientations for the zones with maximum and minimum curvature and thus for the nuclei, it cannot be understood from this point of view why always the same (≈40° <111>) orientation relationship results.

(iii) Since also the Bs-type recrystallization orientation (32$\bar{6}$)[83$\bar{5}$] (in Ref. 30 approximately denoted as (113)[21$\bar{1}$]) lies on a convergent plane, it is concluded[30] that the mechanism of formation of recrystallization texture in materials which twin during deformation (i.e. in those with a Bs-type rolling texture) is essentially the same as in non-twinning materials (i.e. with a Cu-type rolling texture) with the nucleation occurring in this case only in those grains which have not twinned. Then, however, it cannot be understood why in the twinning case the recrystallization textures come out to be radically different from those of the non-twinning case (but again related to the matrix by a ≈40° <111> rotation).

Concerning the present results, the measured Cu- and Bs-type rolling textures were thoroughly examined for indications as to whether or not the nuclei of the observed

recrystallization orientations were part of the deformed matrix. The main components of the recrystallization texture, (001)[100] and (326)[83$\bar{5}$], were not found in the deformed state with any of the techniques used: the consideration of extremely low intensities in the pole figures (0.1 contour-lines), the determination of single grain orientations by electron diffraction measurements,[8] the determination of the three-dimensional ODF given in part.[10]* A positive result was obtained only for the (013)[100] orientation which seemed to occur in the recrystallization texture only if it was also present in the rolling texture. This could be observed in the case of silver (Figures 11a/b and 12a/b). After rolling at room temperature this orientation occurred in both the recrystallization and rolling textures, whereas after rolling at -196°C it occurred in neither. This result could also be obtained by inspection of the ODF.

(b) *Nuclei as twins of first or higher generations of the deformed matrix.* From electron microscopical and X-ray examinations Peters[36] concluded that for a Cu-10%Sn alloy mainly second generation twins acted as nuclei. This is plausible since first generation twins, to a large extent forming slowly migrating coherent twin-boundaries with respect to their matrix, do not have a good chance of growing. The role of twinning for the formation of recrystallization textures is indicated also in the work of Schmidt, Lücke and Pospiech[10] on Cu-P-alloys where all observed components were second generation twins to the matrix. Nucleation by formation of higher generation twins has recently been shown directly by Gottstein et al.[37] for the recrystallization of Cu-single crystals. In this work, however, it was also found that the only twin orientations which grew to a large volume were those which possessed approximately a 30°-40° <111> relationship to the deformed matrix.

The recrystallization texture found by Peters is similar to those observed here for Cu-Zn and Ag and described by (326)[83$\bar{5}$].** The twin orientations to (326)[83$\bar{5}$] shown in Figure 18 where the scatter of the Bs-type rolling texture up to the 1.0 contour is indicated by the hatched region $AB_TC_TD_T$ only 13° away from complementary orientation (362)[8$\bar{5}$3] (AB'C'D'). A second twinning around axis B_T of this first order twin leads to an orientation $A_{TT}B_TC_{TT}D_{TT}$ which is 22° away from (011)[21$\bar{1}$] but situated in the bridge between (011)[21$\bar{1}$] and (011)[100] which is strongly occupied in the Bs- and Tr-type rolling textures (see Figures 3 and 4). In

*In the literature, the observation of nuclei in the deformed matrix has only been reported for the cube orientation.[35] Most authors, however, specifically noted their absence.[34,35] Since in our own experiments the cube orientation was found strongly in some batches of copper rolled at 20°C by 95%, whereas not at all in others, it is suspected that it is the result of an undesired recrystallization.

**The indices (124)[21$\bar{1}$] given by Peters seem to be incorrect. The (124)[21$\bar{1}$] orientation has a distance $\rho = 18°$ from the one shown in his pole figures which is only 4° off (326)[83$\bar{5}$].

contrast, a direct twinning around pole B' of the complementary orientation $(\bar{3}62)[8\bar{5}3]$ AB'C'D' leads to a position 20° away from $(011)[21\bar{1}]$ but outside the spread of the rolling texture. The fact that the second order twin position with respect to $(326)[83\bar{5}]$ is well occupied in the rolling texture, but not the first order position has also been reconfirmed by inspection of the 3-dimensional ODF.

Thus it shall be concluded that the nuclei for the $(326)[83\bar{5}]$ orientation cannot be obtained as first order twins but as second order twins which originate in the spread of the rolling texture at $\rho = 22°$ from $(011)[21\bar{1}]$ in the bridge between $(011)[21\bar{1}]$ and $(011)[100]$. This is supported by the fact that $(326)[83\bar{5}]$ is observed as a recrystallization orientation only if $(011)[21\bar{1}]$ and $(011)[100]$ (and thus also the bridge between) is present in the rolling texture. On the other hand, twin formation cannot be regarded as the sole mechanism determining the orientation of nuclei. Firstly, the frequently observed 40° <111> orientation relationship does not result if only twinning without further selection is assumed.* Secondly, twinning is rather improbable for metals with high stacking fault energy which means that the cube texture which is found with these metals needs another explanation.

(c) *Nuclei generated by the inverse Rowland transformation (IRT)* (eventually followed by twinning. According to Burgers and Verbraak[38] a nucleus of a new orientation can be formed from a rolling orientation and the corresponding twin orientation by IRT. For example, the cube orientation can be obtained from $(112)[11\bar{1}]$ + twin $(112)[\bar{1}\bar{1}1]$ or $(011)[21\bar{1}]$ + twin $(011)[\bar{2}1\bar{1}]$. This mechanism, although questioned by some workers on theoretical grounds,[39] was also indicated by an electron microscope examination of partially recrystallized copper by Hinkel, Haase and Granzer[40] who observed cube grains surrounded by grains and twins of these types. Slakhorst[17] concluded from electron-macroscopic and texture evidence that in silver the nuclei of the final orientations are formed by IRT and subsequent twinning; e.g. $(326)[83\bar{5}]$ as a second generation twin from $(001)[100]$ formed by IRT ($\rho = 9°$) and $(013)[100]$ as a third generation twin from $(012)[210]$ which is also formed by IRT ($\rho = 8°$). The cube texture should arise if the stacking fault energy is so high that no twinning can occur but only IRT. However, the observed preference for the 40° <111> orientation relationship cannot be explained solely by IRT. It must be followed by twin formation at least to the second generation** and from the resulting higher order

*Twinning leads to the following orientation relationships and deviations ρ from the nearest 40° <111>: First order twins: 60° <111>, ρ = 20°; second order twins: 39° <011>, $\rho = 22°$; third order twins: 32° <111>, $\rho = 22°$ and 35° <012>, $\rho = 22°$.

**The following orientation relationships with respect to the matrix and deviations ρ from 40° <111> are obtained. IRT: ≈57° <123>, $\rho = 22°$; IRT + 1, order twin: ≈22° <013>, $\rho = 26°$; IRT + 2. order twin: ≈39° <014>, $\rho = 26°$; ≈22° <135>, $\rho = 18°$ and ≈36° <111>, $\rho = 4°$.

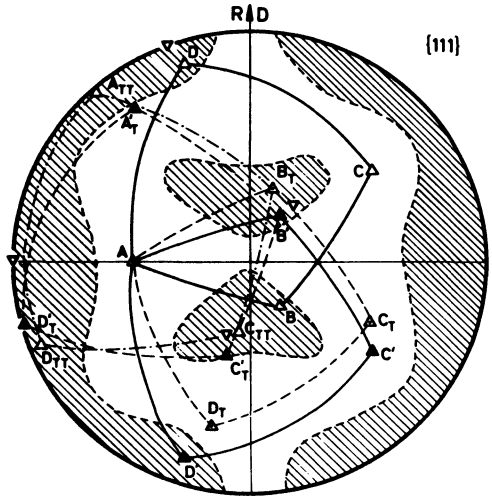

Figure 18. Twin relationships between deformed matrix (∇(011)[21$\bar{1}$], hatched region = intensity 1.0) and brass recrystallization orientation ((326)[83$\bar{5}$]). $\triangle$(full lines) = ABCD = (326)[83$\bar{5}$] (component I); $\blacktriangle$(full lines = AB'C'C' = (362)[8$\bar{5}$3] component II; $\triangle$(dashed lines) = $AB_TC_TD_T$ = first order twin to ABCD; $\triangle$(dashed-dotted lines) = $A_{TT}B_TC_{TT}D_{TT}$ = second order twin of ABCD; $\blacktriangle$ (dashed lines) $A'_TB'C'_TD'_T$ = first order twin of AB'C'D'.

twins only the few ones showing this relationship must be selected.

5.3 *Summary*

Summarizing this discussion, the following statements can be made:

(i) The three possibilities discussed above for the formation of nuclei (nuclei as part of strongly disoriented regions of the deformed matrix, nuclei as higher order twins to differently oriented parts of the matrix and nuclei formed by the inverse Rowland transformation eventually followed by higher order twin formation) do not contradict the results of the present work and might correctly describe mechanisms of nucleation occurring under different circumstances. However, only in a few cases (e.g. formation of (013)[100]) can direct indications be drawn from this work as to which of these mechanisms applies.

(ii) There are two possible definitions of nucleation: the formation of a strain free region capable of growing into the deformed matrix (observable in the electron microscope), and the beginning of the growth of those grains which will become large enough to determine the structure after primary recrystallization (observed in the recrystallization texture). This distinction appears necessary since it is possible that the grains originally formed from the deformed matrix have a very low growth rate thus remaining negligibly small and that the fast

growing grains form only at a later stage of recrystallization. For example, a slowly growing grain nucleated in the deformed matrix by any of the above mechanisms might form a recrystallization twin which grows faster and thus finally assumes a much larger volume than the original grain. This implies that the orientations resulting from the original nucleation within the deformed matrix may not be directly related to the observed recrystallization textures and that, in this example, twinning should be considered to be the true nucleation events for the grains determining the microstructure after primary recrystallization.

(iii) Most orientations found in the recrystallization textures (e.g. (326)[83$\bar{5}$]) are not found in the corresponding rolling texture. This could indicate that the volume fraction of the matrix present in these orientations is too small to be detected, but it could also suggest that nuclei of such orientations are not present in the deformed matrix but are formed only during the process of recrystallization. On the other hand, the intermediate stages in the twin and transformation chains predicted by mechanisms (b) and (c) are, in most cases, not observed either (e.g. the first order twins to (326)[83$\bar{5}$]). This means that, in order to maintain any of the 3 nucleation theories, it is necessary to assume that certain orientations are present but in unobservably small amounts. This is an additional difficulty in distinguishing between the different mechanisms. Only in some single crystal work (e.g. Zabardjadi et al. on Cu [41]) have the twin chains really been demonstrated in detail.

(iv) The 3 nucleation processes above do not seem capable of explaining the observed ≈40° <111> orientation relationship between the main recrystallization components and the deformed matrix without additional assumption. Mechanism (a) (preformed nuclei) could do so apparently only for the cube orientation, mechanism (b) (twinning) not at all and (c) (IRT) only if additional higher order twinning is assumed (and even then only in a few of many possibilities). This and the fact that the 40° <111> relationship is identical with the maximum growth rate relationship strongly suggest that this relationship is determined by oriented growth. It would mean that one or several of the discussed nucleation mechanisms are making available nuclei of many different orientations (but possibly not of all orientations) from which the recrystallization orientations are selected by preferred growth. This is supported by the observation that the recrystallization textures are often even sharper than the rolling textures, which indicates that not only a simple orientation transformation but an additional selection process takes place. Again this can be explained by oriented growth (in cases of compromise growth) but not by the nucleation: Mechanisms (b) and (c) lead to many different orientations while mechanism (a) may lead to a few sharp orientations but apparently not to the observed ones.

(v) It is difficult to decide whether the fact that orientations apparently favourably oriented for growth are not observed, whereas less favourable orientations occur, is a result of additional growth inhibitions or missing nucleation. For example, the complete absence of the orientations (211)[01$\bar{1}$] in the Bs-type recrystallization texture has been interpreted as growth inhibition due to the Goss orientation. It could, however, also be interpreted in terms of a lack of nuclei of this orientation: it is not present in the deformed matrix (in contrast to (013)[100]), it is not a second generation twin with respect to the deformed matrix (in contrast to (326)[83$\bar{5}$]), it cannot be formed by IRT (in contrast to (001)[100]) and it cannot be formed by IRT and subsequent twinning (in contrast to (326)[83$\bar{5}$]). In this case the main influence of nucleation on the recrystallization texture would be that not all orientations capable of fast growth are nucleated.

ACKNOWLEDGEMENTS

The authors would like to thank Prof. I. L. Dillamore for lively discussions which were greatly conducive to achieving the aims of this work, Dipl.-Ing. K. H. Virnich for valuable discussions and help in preparing the manuscript, and Dr. G. Frommeyer for contributing some careful experiments. They acknowledge the financial support by the Ministerium für Wissenschaft und Forschung des Landes Nordrhein-Westfalen.

REFERENCES

1. e.g. G. Wassermann and J. Grewen, *Texturen metallischer Werkstoffe*, 2. Aufl. (Springer-Verlag, Berlin/Göttingen/Heidelberg, 1962).
2. R. Alam, H. D. Mengelberg and K. Lücke, *Z. Metallkde.*, 58, 867 (1967).
3. U. Kobbe and H. Schuon, *Siemens Z.*, 47, 119 (1973).
4. L. G. Schultz, *J. Appl. Phys.*, 20, 1030 (1949).
5. B. F. Decker, E. T. Asp and D. Harker, *J. Appl. Phys.*, 19, 388 (1948).
6. H. D. Mengelberg, M. Meixner and K. Lücke, *Acta Met.*, 13, 835 (1965).
7. F. Rosenbaum, Doctor-Thesis, TH Aachen (1971).
8. H. Perlwitz, K. Lücke and W. Pitsch, *Acta Met.*, 17, 1183 (1969).
9. J. Pospiech and K. Lücke, *Acta Met.*, 23, 997 (1975).
10. U. Schmidt, K. Lücke and J. Pospiech, in *Texture and the Properties of Materials*, Proc. of the 4th International Colloquium on Texture, Cambridge 1975 (The Metals Society, 1976, p. 147).
11. H. Hu, R. S. Cline and S. R. Goodman, *J. Appl. Phys.*, 32, 1392 (1961).
12. A. Merlini and P. A. Beck, *Trans. AIME*, 203, 385 (1955).
13. P. A. Beck and H. Hu, *Trans. AIME*, 194, 83 (1952).
14. K. Lücke and U. Schmidt, *J. Less-Common Metals*, 28, 187 (1972).

15. H. Hu and S. R. Goodman, *Trans. Met. Soc. AIME*, 227, 627 (1963).
16. H. Hu, R. S. Cline and S. R. Goodman, *Trans. Met. Soc. AIME*, 226, 96 (1962).
17. J. W. H. G. Slakhorst, *Acta Met.*, 23, 301 (1975).
18. R. H. Richman and Y. C. Liu, *Trans. Met. Soc. AIME*, 221, 720 (1961).
19. P. A. Beck, *Acta Met.*, 1, 230 (1953); P. A. Beck, P. R. Sperry and H. Hu, *J. Appl. Phys.*, 21, 420 (1950).
20. G. Ibe and K. Lücke, in *Recrystallization, Grain Growth and Textures*, Ed. H. Margolin (ASM, Metals Park, Ohio, 1966),p. 434.
21. G. Ibe, W. Dietz, A. C. Fraker and K. Lücke, *Z. Metallkde.*, 61, 498 (1970).
22. B. Liebmann, K. Lücke and G. Masing, *Z. Metallkde.*, 47, 57 (1956).
23. P. A. Beck, in *The Physics of Powder Metallurgy* (McGraw-Hill Book Co., New York 1951), p. 40; Y. C. Liu and W. R. Hibbard, Jr., *Trans. AIME*, 197, 672 (1953); A. Merlini and P. A. Beck, *Acta Met.*, 1 598 (1953).
24. P. A. Beck, *Advances in Physics (Phil. Mag. Sup.)*, 3, 245 (1954).
25. K. Lücke, R. Rixen, F.-W. Rosenbaum, in *The Nature and Behavior of Grain Boundaries*, Ed. H. Hu (Plenum Publishing Corp., New York, 1972), p. 245; K. Lücke, *Can. Met. Quart.*, 13, 261 (1974); K. Lücke, *Journal de Physique*, 36, C4-339 (1975).
26. G. Ibe and K. Lücke, *Texture*, 1, 87 (1972).
27. P. A. Beck and H. Hu, in *Recrystallization, Grain Growth and Textures*, Ed. H. Margolin (ASM, Metals Park, Ohio, 1966), p. 393.
28. I. L. Dillamore, *Acta Met.*, 12, 1005 (1964).
29. W. G. Burgers and P. C. Louwerse, *Z. Physik*, 61, 605 (1931).
30. I. L. Dillamore and H. Katoh, *Metal Sci.*, 8, 73 (1974).
31. K. Lücke, R. Rixen and M. Senna, *Acta Met.*, 24, 103 (1976).
32. J. Hansen, H. Mecking and K. Lücke, *Acta Met.*, 24, 633 (1975).
33. M. Senna and K. Lücke, *Z. Metallkde.*, 67, 752 (1976)
34. F. Haessner, U. Jakubowsky and W. Wilkens, cf., e.g. *Mat. Sci. Eng.*, 1, 30 (1966); H. Perlwitz, K. Lücke and W. Pitsch, in Ref. 8.
35. H. Hu, *Reorientations in Recrystallization: Origin of the Cube Grains in Copper - A Study of Nucleation in Recrystallization*, in *Texturen in Forschung und Praxis*, Ed. J. Grewen, G. Wassermann (Springer-Verlag, 1969), p. 200.
36. B. F. Peters, *Met. Trans.*, 4, 757 (1973).
37. G. Gottstein, H. Mecking and D. Zabardjadi, *Proc. Int. Conf. Strength of Metals and Alloys 4*, Nancy (1976), p. 1126 (Vol. III).
38. W. G. Burgers and C. A. Verbraak, *Acta Met.*, 5, 765 (1957); C. A. Verbraak, *Acta Met.*, 6, 580 (1958).
39. J. Christian, private communication.

40. H. Hinkel, G. Haase and F. Granzer, *Acta Met.*, 15, 1875 (1967).
41. D. Zabardjadi, Thesis, TH Aachen (1976).